https://doi.org/10.2352/EI.2022.34.9.IQSP-357

Updated Camera Spatial Frequency Response for ISO 12233

Peter D. Burns[1], Kenichiro Masaoka[2], Kenneth Parulski[3], and Dietmar Wueller[4]
[1]Burns Digital Imaging, [2]NHK Science and Research Labs., [3]aKAP Innovation, LLC., [4]Image Engineering GmbH & Co.KG

Abstract

The edge-based Spatial Frequency Response (e-SFR) method is well established and has been included in the ISO 12233 standard since the first version in 2000. A new 4th edition of the standard is proceeding, with additions and changes that are intended to broaden its application and improve reliability. We report on results for advanced edge-fitting which, although reported before, was not previously included in the standard. The application of the e-SFR method to a range of edge-feature angles is enhanced by the inclusion of an angle-based correction, and use of a new test chart. We present examples of the testing completed for a wider range of edge test features than previously addressed by ISO 12233, for near-zero- and -45-degree orientations. Various smoothing windows were compared, including the Hamming and Tukey forms. We also describe a correction for image non-uniformity, and the computing of an image sharpness measure (acutance) that will be included in the updated standard.

Introduction

The edge-based Spatial Frequency Response (e-SFR) method that is part of the current ISO 12233:2017[1] standard has its roots in edge-gradient analysis of optical and photographic systems.[2,3] The method was adapted to use slanted, or rotated edge features[4] in the first edition of the standard for digital camera resolution. Since then, the method has been applied in a wide range of applications including, photographic scanners[5], medical x-ray[6], mobile imaging,[7] and archiving[8] systems. This has led to several changes aimed at improving accuracy and reliability.

Many other international standards and best-practice guidelines refer to this method. Therefore, changes in the ISO 12233 method can influence the development of these other efforts. The intent is that by describing these details, other image-quality related activities will be helped as they consider whether and how to adopt the new components of ISO 12233 edition 4 in their standards and guidelines.

We should point out that the standard includes two other methods for camera resolution evaluation, using sinewaves[9] (s-SFR), and visual resolution. However, here we limit our discussion to specific changes and additions that apply to the e-SFR measurement method.

e-SFR Method

Although detailed elements of the method are given in the standard, and elsewhere, several basic steps are shown in Fig. 1. Based on an array of image data corresponding an edge-feature, an edge profile is computed in the direction across the edge. This involves detection of location and slope of the edge, and projection of the image pixel values along the edge to form the edge profile vector. This is accomplished by binning (accumulating) the values in a (4x) super-sampled function. This edge profile is interpreted as the Edge Spread Function (ESF).

This edge profile is used to compute an equivalent line-spread function via a derivative operation ($ESF' = dESF/dx$). Since we are working with sampled data, this is done using a digital filter in the second step. A window function is then applied to this vector. This has the effect of smoothing the resulting e-SFR.

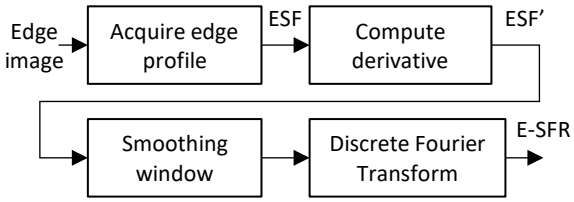

Figure 1: Major steps for e-SFR analysis

The final operation is the computing of the Discrete Fourier Transform (DFT) of this windowed array. The modulus of the resulting array is then normalized (scaled) to unity at zero-frequency. This e-SFR is often referred to as a measurement of the presampled Modulation Transfer Function (MTF) of the system. While a detailed discussion if this is beyond our scope here, it may be helpful to explain several points.

Historically the MTF was defined, e.g., for an optical system, as the modulus of the Fourier transform of the point-spread function. Several methods have been developed for MTF measurement, one being edge-gradient analysis. Others include those based on sinusoidal and random-noise images.

In this paper, we refer to the ISO 12233 slanted-edge method as the edge-spatial frequency response (e-SFR), as does the standard. We can often interpret the e-SFR as a measurement (or estimate) of the presampled MTF based on the ISO 12233 method. However, we use 'SFR' rather than 'MTF' since digital cameras are usually not linear systems due to, e.g., sampling, color-filter interpolation, and non-linear image processing. As with any measurement, the e-SFR can be subject to error in the form of both variation and bias.

Updated ISO 12233

Several changes and additions will be included in the 4th edition of the standard. The original e-SFR method was aimed at, and restricted to, evaluating near-vertical and near-horizontal edge features. In the updated version, a wide range of edge-angles are included. In addition, in earlier versions of ISO 12233, these edges were assumed to be straight and undistorted. Accommodations for spatial distortion of the measurement edge are included in the updated standard. We now describe these and other changes, addressing improved accuracy, robustness, and additional measures.

SFR Correction for Derivative Filter

This correction was first included in the 2nd edition in 2014, but the Annex showing the derivation of the correction is newly added in the 4th edition. The first derivative of the edge profile is computed using a three-point digital filter, the central difference, in the second step of Fig. 1. For input vector (edge profile), x, the output line-spread function vector, y, is computed as

$$y_n = 0.5(x_{n+1} - x_{n-1}). \quad (1)$$

This filter approximates the derivative operation, but imposes an unwanted 'frequency response', when compared to an ideal first derivative. This is described in general by Hamming,[10] and in reference to e-SFR evaluation in Ref. 11. This response is shown in Fig. 2.

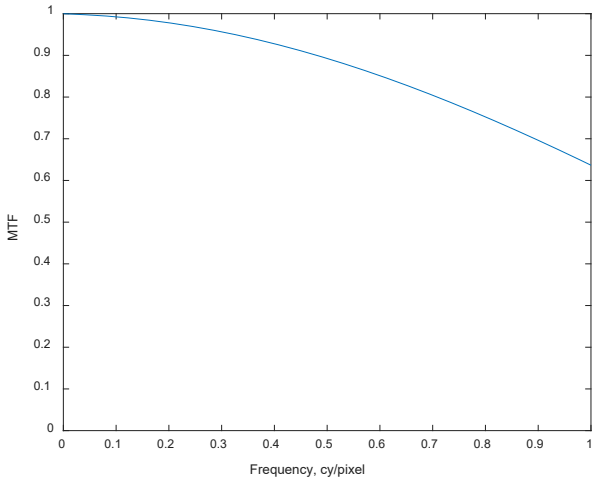

Figure 2: MTF due to the central difference derivative filter

As can be seen, this introduces a moderate attenuation (negative bias) at high frequencies. It is corrected in the frequency domain by multiplying the computed e-SFR by the inverse of this function. The form of the correction, T_{deriv}, is

$$T_{deriv}(u) = \frac{2\pi\delta u}{\sin(2\pi\delta u)}, \tag{2}$$

where u and δ are the spatial frequency and data sampling interval, respectively.

SFR Correction for Edge Angle

One way to describe the generation of the super-sampled edge profile is to consider it as a projection of the edge (or averaging) in the direction along the edge. When the image data are accumulated at locations, *i.e.*, sampled, at intervals of 0.25 pixel, this also defines the spatial frequency values for the resultant e-SFR. Since the 0.25-pixel sampling applies along the pixel direction (for a vertical edge), this is not the corresponding sampling interval for a profile *normal to* the edge.

Figure 3 shows this condition, where $\overline{AB}$ is the pixel binning distance, 0.25 pixel. If we interpret the edge profile as normal to the edge, however, we see that *this* bin-sampling interval is $\overline{AC}$. If the original sampling interval is $\delta = \overline{AB}$ then the effective edge profile sampling interval normal to the edge is $\delta_{corr} = \overline{AC}$. These can be related via the edge angle and the corrected edge profile, which is given by[12]

$$ESF_{corr}(x) = ESF(x/\cos\,\theta). \tag{3}$$

We can accomplish this by interpreting the sampling interval for the edge profile, and its derivative, as

$$\delta_{corr} = \delta\,\cos\theta. \tag{4}$$

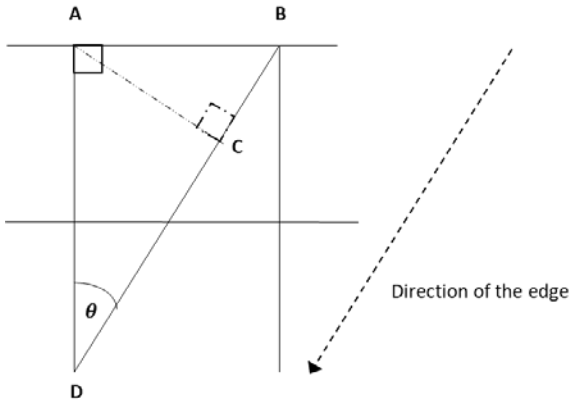

Figure 3: Sampling of the edge profile normal to the edge feature

This correction results in the following adjustment to the spatial frequency values for the e-SFR result,

$$SFR_{corr}(u) = SFR(u\,\cos\theta). \tag{5}$$

An example is shown in Fig. 4, for a 30-degree edge angle.

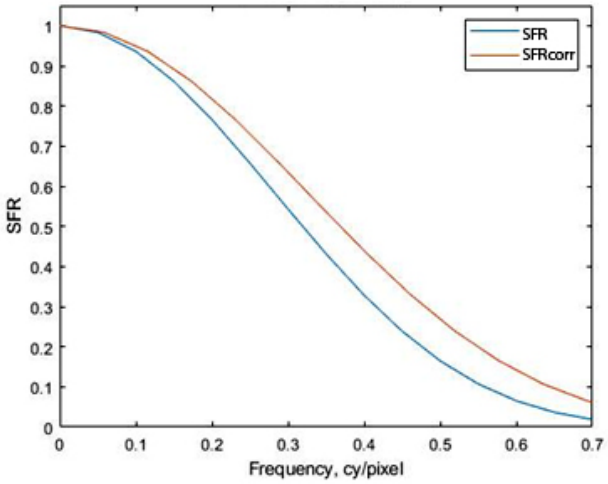

Figure 4: Example of uncorrected and Edge-Angle corrected e-SFR results for 30-degree edge

Advanced Edge-Fitting

Edge-gradient analysis is generally based on the images of straight edge-features, and this was true for the previous editions of ISO 12233. Straight edges were required in the test object and assumed in the captured test images. However, in several practical applications, the image edge-feature will be subject to distortion. For example, with various optical distortions the edge will be curved.

This causes a reduction in the e-SFR due to an effective widening of the estimated edge profile.[13] In this situation, we have two characteristics interacting. The curvature of the edge (distortion) is introducing (bias) error into the e-SFR measurement.

In some cases, this situation can be mitigated by reducing the size (height for a vertical edge) of the analysis region of interest (ROI). However, this can lead to increased variation error due to image noise since fewer data are being accumulated (averaged) along the edge.

One way to decouple the distortion from the edge micro-structure is to apply a polynomial, rather than a linear model to the edge location data.[13]

$$x = a_0 + a_1 y + a_2 y^2 + a_3 y^3 \cdots \quad (6)$$

This equation is written as $f(y)$ rather than the more common $f(x)$ because the edge x-location is computed line-by-line as part of the slanted-edge analysis. This edge fitting and correction has been addressed as part of a multi-order selection[14] scheme, and as applied to optical design.[15] For the new 4th edition of ISO 12233 the use of a 5th order polynomial is recommended, with lower-order fitting being acceptable, but noted when reporting e-SFR results.

One concern with higher-order edge fitting was that image noise can introduce error in the form of over-fitting. While this can happen, of course, testing of camera images did not reveal this to be a common or serious problem. As an example, Fig. 5 shows a barrel-distorted camera image. The e-SFR was computed for a near 26-degree edge, based on a 60 x 40 pixel ROI, as shown in the upper right quadrant. The test chart used here is the new preferred test chart for measuring e-SFR, documented in the new 4th edition of ISO 12233.

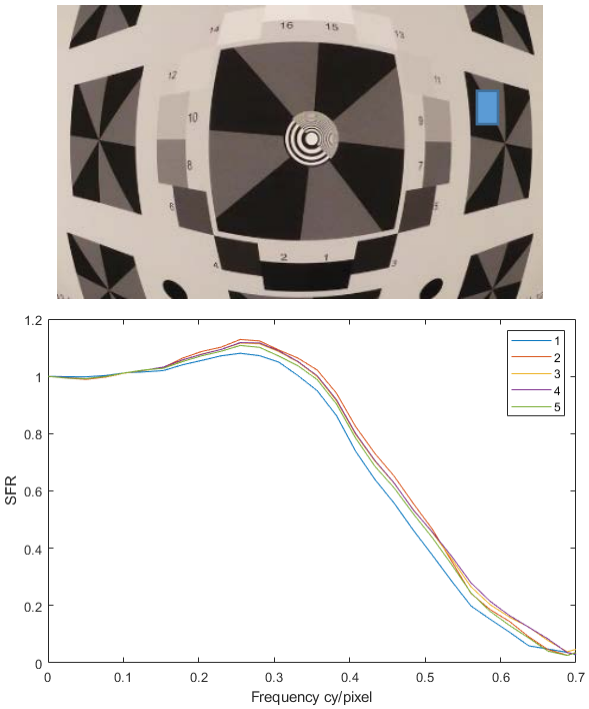

Figure 5: Barrel-distorted test chart image for a consumer camera, ISO 800, and results for 26-degree edge angle. The blue rectangle indicates the ROI.

In this case consistent, and acceptable, results were obtained for 2nd through 5th -order edge-fitting. For a larger ROI, we would expect more curvature within the ROI, and greater variation. We conclude that the polynomial edge fitting can effectively reduce or eliminate the influence (bias) caused by spatial distortion.

It should be noted that the polynomial edge-fitting can also be used to evaluate intentionally curved edge features. Although not part of the updated ISO 12233 standard, the use of 'pie' (concentric circular) features was demonstrated in Ref. 15. In this case the curved edge-fitting is required.

Window Carpentry†

The choice of a signal-processing window is best known in detection tasks, when it is applied to narrow-band signals, such as sinewaves. The length (duration) of the input data, combined with any applied window (apodization) function results in a window 'spectral response' being introduced. When viewed in the frequency domain, as we do with the e-SFR, this introduces a smoothing operation. By Fourier transform properties, the computed SFR is convolved (filtered) by the Fourier transform of the window function. Since we do not assume any underlying functional form of the SFR or image noise, the choice of window function was made based on investigation rather than derived.

The current version, ISO 12233:2017, uses a Hamming window to smooth the computed e-SFR. The application of the window is a point-by-point multiplication by the window coefficients, in the third step of Fig. 1. The reason for smoothing the e-SFR is to reduce the influence of image noise.

The Tukey window is now being substituted for the Hamming window and can also be expected to provide a smoothing effect. This window was considered because it has a zero-value at its endpoints. The rationale was that for ROIs with left-to-right non-uniformity, suppressing the end values could reduce any low-frequency discontinuity that may be introduced. We might also expect that the shape would be more important for narrow ROIs.

This window has a parameter whose selection provides the chance to select the shape of the window, and therefore the nature (amount) of the smoothing. Here we investigate the use of the parameter, α [0-1] illustrated in Fig. 6. As shown, the higher the value of alpha, the narrower the window, and the more smoothing we can expect.

The choice of window function was found to have little effect on the resulting e-SFR. This was particularly true for computed, noise-free edges, whose near-identical results are not presented here. To evaluate the influence in the presence of noise, edge-image arrays were computed, following the method described in Ref. 16. Edges with a known edge profile (SFR) were generated for various angles. Following this, stochastic noise was added. In this window-study, all other conditions and corrections used in the new ISO 12233 method were applied.

Figure 7 shows results for a 44-degree edge, with correlated noise added. The noise had a standard deviation of 10, on a [1-255] scale, and a three-pixel correlation. The ROI size was 100x100 pixels. We observe that the results are consistent with the ideal (noise-free) computed $\mathrm{sinc}^4(u)$ form.

As a second example, consider the results for a Nikon D7500 camera with an ISO setting of 10,000, for a 5-degree edge, and a small (75 pixels) width ROI. Figure 8 shows the computed e-SFR for several window shapes. For the Tukey window we observe a modest variation in the amount of spectral smoothing, generally increasing with the parameter, α.

Following these and other results, a value of $\alpha = 1.0$ was selected for the updated standard. This is a special case of the Tukey window, called a Hann window.

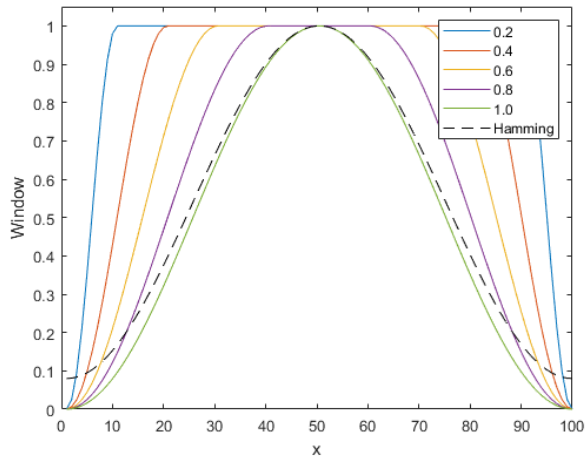

Figure 6: Variation of Tukey window with shape parameter, α, and Hamming window used in previous editions of the standard

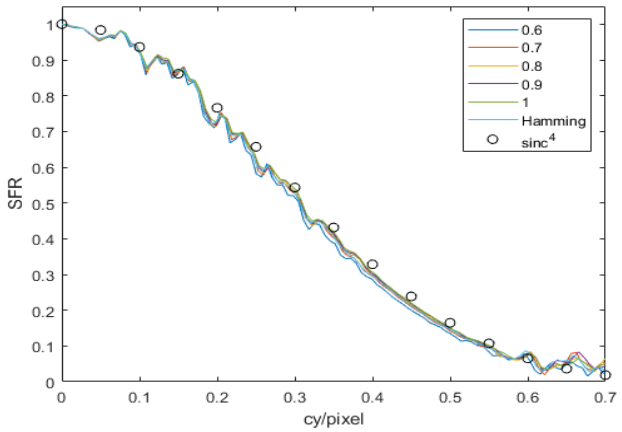

Figure 7: SFR results for a 44-degree computed edge, with image noise added and various window shapes. The numbers are Tukey α values.

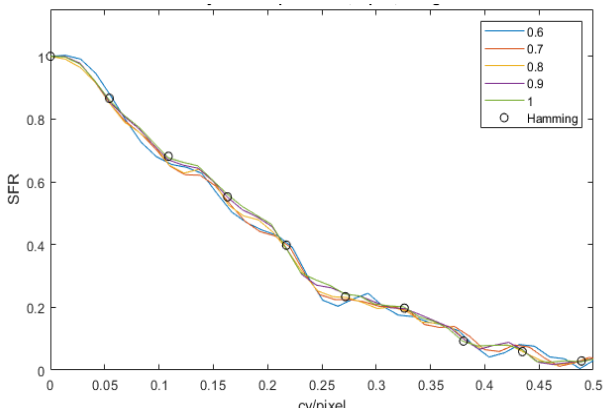

Figure 8: Results for a Nikon D7500 camera with various window shapes

Informative Additions

Several informative sections have been added to the 4th edition of ISO 12233. These include more detailed descriptions of the corrections discussed above. Two more stand out.

Uniformity Correction

We have previously discussed how the e-SFR method has been modified to mitigate the confounding effect of optical distortion. Similarly, optical vignetting and other types of non-uniform illumination can cause problems for this type of evaluation. As discussed in Ref. 15, non-uniform illumination from a lens can increase the computed e-SFR by effectively sharpening the edge, if light fall-off is away from the edge. It can also reduce the e-SFR if the fall-off appears to reduce the edge contrast.

Koren and Koren[17] suggest an approximate correction. Their method fits the light region of the computed edge profile with a polynomial (usually linear) function and subtracts this function. Figure 9 shows an example from Ref. 15 for a computed simulation of a fish-eye lens. We applied the uniformity correction to both sides of the edge. The *x*-axis is in units of the super-sampled edge profile, for a sampling distance 0.25 times the input data sampling. Since this is from an optical simulation, these data do not correspond to camera pixels.

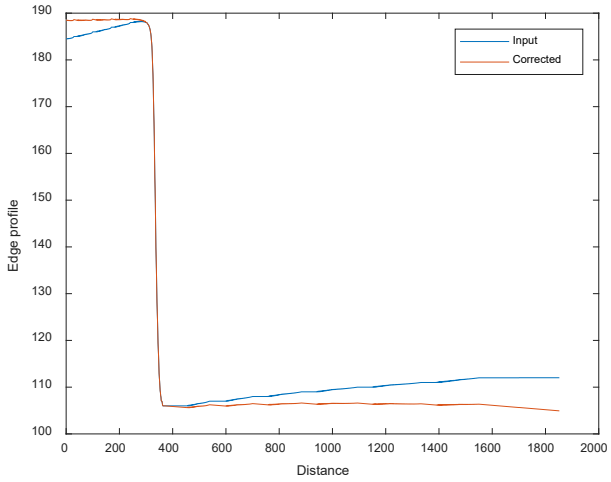

Figure 9: Edge profile derive from simulated fisheye lens design, from Ref. 15

Figure 10 shows the resulting e-SFR, where the non-uniformity across the edge introduces a positive bias at low-frequencies. This bias is reduced when the non-uniformity correction is applied to the lighter side of the edge. When the dark side is also corrected, the bias is further reduced.

This correction method is presented as an optional, informative, rather than a normative part of the standard. We advise using it with care, since the effect can vary with ROI width.

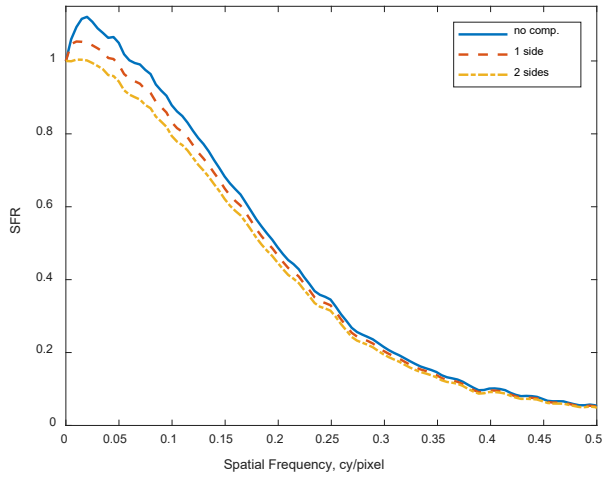

Figure 10: Computed e-SFR results with and without non-uniformity compensation for the case shown in Fig. 9

Acutance

The current ISO standard (12233:2017) includes a measure that is computed from the e-SFR result, the sampling efficiency.[18] This is based on the 10% e-SFR frequency, when compared to the half-sampling, or Nyquist, frequency. The 10% measure is used as an indication of the limiting resolution of the system. The new edition includes an additional measure which is also computed from the e-SFR, acutance. This is a well-established measure, intended to be an indication of the image sharpness that an imaging system can deliver.

The computation of acutance involves integrating (summing) the SFR over spatial frequency, weighted by a visual contrast-sensitivity function. A viewing distance needs to be selected to relate the cy/pixel (or cy/mm) frequency values to the corresponding visual cy/degree. More details on this measure are given in the second paper describing the continuing development of ISO 12233, at this conference.[19]

Conclusions

Several changes to the ISO 12233:2017 standard for evaluating camera resolution have been described. They are aimed at broadening the application of the standard in several ways. By including both polynomial edge fitting and non-uniformity compensation, the method is less susceptible to both geometric distortion and vignetting. In addition, the edge-angle correction is intended to improve the results for a wider range of edge angles than previously included.

Matlab code for e-SFR analysis is available from the ISO, and directly at
http://burnsdigitalimaging.com/iso12233-sfrmat5/

Acknowledgement

It is a pleasure to acknowledge the helpful discussions and input from other members of the ISO/TC42/WG18 standards working group.

References

[1] ISO 12233:2017, Photography—Electronic still picture imaging—Resolution and spatial frequency responses, ISO, 2017.

[2] R. A. Jones, An Automated Technique for Deriving MTFs from Edge Traces, Photogr. Sci. Eng., 11, pp. 102-106 (1967).

[3] J. C. Dainty and R. Shaw, Image Science, Academic, NY, ch. 5. 1975.

[4] S. E. Reichenbach, S. K. Park and R. Narayanswamy, Characterizing Digital Image Acquisition Devices, Opt. Eng., 30, pp. 171-177, 1991.

[5] ISO 16067-1:2003, Photography – Spatial resolution of electronic scanners for photographic images – Part1: Scanners for reflective media, ISO, 2003.

[6] E. Samei and M. Flynn, A Method for Measuring the Presampled MTF of Digital Radiographic Systems Using an Edge Test Device, Med. Phys., 25, pp. 102-113, 1998.

[7] U. Artmann, VCX Version 2020 - Further development of a transparent and objective evaluation scheme for mobile phone cameras, Proc. IS&T International Sym. on Electronic Imaging, Image Quality and System Performance XVIII, IQSP-204, 2021.

[8] FADGI Still Image Working Group, ed. T Rieger, US Library of Congress, http://www.digitizationguidelines.gov/

[9] C. Loebich, D. Wueller, B. Klingen, and A. Jaeger, Digital Camera Resolution Measurement Using Sinusoidal Siemens Stars, Proc. SPIE, Digital Photography III, vol. 6502, 65020N, 2007.

[10] R. W. Hamming, Digital Filters, 3rd Edition, Prentice Hall, pp. 50-53, 1989.

[11] P. D. Burns, Slanted-Edge MTF for Digital Camera and Scanner Analysis, Proc. PICS Conf., IS&T, 135-138, 2000.

[12] J. K. M. Roland, A Study of Slanted-edge MTF Stability and Repeatability, Proc. SPIE, Image Quality and System Performance XII, vol. 9396, 93960L 2015.

[13] P. D. Burns and D. Williams, Camera Resolution and Distortion: Advanced Edge Fitting, Proc. IS&T International Sym. on Electronic Imaging, Image Quality and System Performance XV, IQSP-171, 2018.

[14] V. Cardei, B. Fowler, S. Kavusi, and J. Phillips, MTF Measurements of Wide Field of View Cameras, Proc. IS&T International Sym. on Electronic Imaging, Digital Photography and Mobile Imaging XII, DPMI-006, 2016.

[15] P. D. Burns, D. Williams, J. Griffith, H. Hall, and S. Cahall, Application of ISO standard methods to optical design for image capture, Proc. IS&T International Sym. on Electronic Imaging, Image Quality and System Performance XVII , IQSP-240, 2020.

[16] K. Masaoka, Accuracy and Precision of Edge-based Modulation Transfer Function Measurement for Sampled Imaging Systems, IEEE Access, vol. 6, pp. 41079-41086, 2018.

[17] H. Koren and N. Koren, Correcting Nonuniformity in Slanted-Edge MTF Measurements, Imatest LLC website http://www.imatest.com/2018/08/edge-mtf-nonuniformity

[18] P. D. Burns and D. Williams, Sampling Efficiency in Digital Camera Performance Standards, Proc. SPIE, Image Quality and System Performance V, vol. 6808, 680805, 2008.

[19] K. Parulski, D. Wueller, P. D. Burns, and H. Yoshida, Creation and Evolution of ISO 12233, the International Standard for Measuring Digital Camera Resolution, Proc. IS&T International Sym. on Electronic Imaging, Image Quality and System Performance XIX, 2022 (in press).

Author Biographies

Peter Burns is a consultant for imaging system evaluation, modeling, and design. Previously he worked for Carestream Health, Xerox, and Eastman Kodak. A frequent speaker at technical conferences, he has taught imaging courses for clients and universities for many years.

Kenichiro Masaoka is a Principal Research Engineer at NHK Science & Technology Research Laboratories, Tokyo, Japan. His research interests include color science and digital imaging systems. In 2017, he received the Soc. for Information Display's Special Recognition Award for his contributions to wide-color-gamut UHD-TV display systems and gamut-area metrology.

Ken Parulski joined Kodak Research Labs after receiving electrical engineering degrees from MIT in 1980 and retired as Chief Scientist and Research Fellow in 2012. He is now a consultant to numerous mobile imaging companies and chairs the US IT10 group responsible for ANSI and ISO digital photography standards. He has been project leader for ISO 12233 since its inception in 1992.

Dietmar Wueller studied photographic technology at the Cologne University of applied sciences. He is the founder of Image Engineering, an independent test lab that tests cameras for several publications and manufacturers. He is the German chair of the DIN standardization committee for photographic equipment and active in ISO, IEC, VCX, IEEE and other standardization activities.

---

† Using *Window Carpentry* is our nod to J. W. Tukey, who coined this and many other terms in statistics and time-series analysis.